JOURNAL OF PHYSICAL ORGANIC CHEMISTRY
J. Phys. Org. Chem. 2005; **18:** 918–928
Published online 13 April 2005 in Wiley InterScience (www.interscience.wiley.com). DOI: 10.1002/poc.918

Spectroscopic (Raman, FT-IR and NMR) and theoretical study of alkali metal picolinates

W. Lewandowski,[1]* G. Świderski,[1,2] R. Świslocka,[1] S. Śojtulewski[2] and P. Koczoń[3]

[1] Department of Chemistry, Bialystok Technical University, Zamenhofa 29, 15-435 Bialystok, Poland
[2] Department of Chemistry, University at Bialystok, Hurtowa 1, 15-900 Bialystok, Poland
[3] Department of Chemistry, Warsaw Agricultural University, Nowoursynowska 159 C, Warsaw 02-728, Poland

Received 28 August 2004; revised 30 December 2004; accepted 17 February 2005

ABSTRACT: The FT-IR, FT-Raman and ^{1}H and ^{13}C NMR spectra of lithium, sodium, potassium, rubidium and caesium picolinates were recorded, assigned and compared in the $Li \rightarrow Na \rightarrow K \rightarrow Rb \rightarrow Cs$ series and analysed. Experimental, vibrational and NMR spectra were interpreted with the aid of calculated data from density functional theory at the B3PW91/6–311++G** level. Distance, angles and dipole moments and also aromaticity indices (*HOMA*, *EN*, *GEO*, I_6) for the optimized structures of picolinic acid and sodium picolinate were calculated. Comparison of theoretical and experimental (x-ray) data and the application of Bader's theory enabled us to evaluate the intramolecular interactions in picolinic acid. Also, the influence of the carboxylic anion structure and the nature of metal–ligand bonding on the electronic charge distribution in the aromatic ring was investigated. The degree of perturbation in the electronic system of the ligand under the influence of metal in the $Li \rightarrow Cs$ series was investigated with the use of statistical methods (principal component analysis) and calculated aromaticity indices.

KEYWORDS: picolinates; Raman spectra; FT-IR; NMR; electronic system; aromaticity indices; *ab initio* calculations, Bader's theory

INTRODUCTION

In our previous work,[1–3] the electronic structure of pyridinecarboxylic acid (isonicotinic and nicotinic acids) derivatives and their complexes with selected metals were studied. The ligands were treated as models to study enzymes and other biologically important molecules. Preliminary results of our earlier investigations allowed us to draw the interesting conclusion that there is a correlation between the position of the metal in the periodic table and the degree of electronic charge distribution or stabilization in the ligands studied. Alkali elements and heavy metals, such as Hg(I), Hg(II), Pb(II), Cd(II) and Ag(I), perturb the electronic system of ligands, whereas 3d, 4f transition metals, e.g. Cr(III), Fe(III), Zn(II) and Ln(III), and Al(III) stabilize it. In the case of these metals stabilization of the electronic system of the ligands increases with decrease in the ionic radius of the central ion.[4–6] An increase in the ionic radius of the central ion, and a decrease in ionic potential (defined as the charge to radius ratio), results in an increase in the perturbation of the electronic system of the ligand.[4,7]

**Correspondence to:* W. Lewandowski, Department of Chemistry, Bialystok Technical University, Zamenhofa 29, 15-435 Bialystok, Poland. E-mail: w-lewando@wp.pl
Contract/grant sponsor: Polish State Committee for Scientific Research; *Contract/grant number:* 6 PO6T 08521.
Contract/grant sponsor: Bialystok Technical University; *Contract/grant numbers:* W/IIS/31/03 and I/IIŚ/24/04.

Further, from our previous work on transition metal complexes,[4,5] it follows that there is a relationship between the delocalization of the electronic charge in the aromatic ring and in carboxylic anion and the delocalization of f orbitals in coordinated lanthanide ions. An increase in delocalization of f orbitals in central ions is followed by an increase in delocalization of electronic charge in the carboxylic anion and the aromatic ring.[8–10]

The aims of the present work were as follows:

1. to investigate the correlation between the vibrational structure (spectroscopic study) and the electronic charge distribution in the aromatic ring, carboxylic anion and the metal ion;
2. to establish the theoretical structures of the studied compounds (calculation of the bond lengths and angles, dipole moments and aromaticity indices) and to compare them with the real structures, allowing for the intermolecular effects. Collection of new data on the geometry and electronic structure of the studied complexes will contribute to the study of the molecular mechanisms of metal-induced perturbation or stabilization of the electronic structure.

A further aim was to gather missing spectroscopic data on alkali metal picolinates, from FT-IR, FT-Raman and NMR (^{1}H, ^{13}C) studies. Available data on these compounds are fragmentary and come mainly from the

Raman spectra of picolinic acid.[11] In the literature, there is a lack of any IR, Raman and NMR spectral data on rubidium and caesium picolinates.

To accomplish the above aims, it will be helpful to use, in addition to the experimental data, also calculations of aromaticity indices and quantum calculations for evaluation of structure and electronic charge distribution.

In this work we examined a new set of compounds, namely lithium, sodium, potassium, rubidium and caesium picolinates. Picolinic acid and its complexes with alkali metals were thoroughly investigated by different experimental (IR, Raman, NMR) and theoretical (B3PW91, B3LYP, HF) methods.

Picolinic acid (PA) is a very interesting model, as it is a biologically important ligand incorporated into some enzymes and its molecule is an active agent in some drugs. The structures, chemical properties and biological activities of picolinic acid and metal complexes of picolinates have been widely investigated.[12–19] PA is the body's prime natural chelator of vital trace elements: chromium, zinc, manganese, copper, iron and molybdenum. Biosynthesized in the liver and kidneys from the amino acid tryptophan, and stored in the pancreas during digestion, PA is secreted into the intestine. PA is present in dietary additives as a carrier of the divalent zinc or chromium cation and these compounds are widely distributed and consumed.[20]

EXPERIMENTAL AND THEORETICAL CALCULATIONS

The alkali metal picolinates were obtained by dissolving PA powder in an aqueous solution of the appropriate base in a stoichiometric ratio. Elemental analysis showed that the metal-to-ligand ratio was 1:1. The results of elemental analysis for sodium picolinate are %C = 49.6 (theoretically 49.7), %H = 2.5 (theoretical 2.8), %N = 9.5 (theoretical 9.6) and %Na = 15.6 (theoretical 15.8). The IR spectra were recorded with an Equinox 55 spectrometer within the range 400–4000 cm^{-1}. Samples in the solid state were measured in a KBr matrix; pellets were obtained with a hydraulic press under 739 MPa pressure. Raman spectra of solid samples in capillary tubes were recorded in the range 400–4000 cm^{-1} with an FT-Raman accessory of a Perkin-Elmer 2000 system. The resolution of the spectrometer was 1 cm^{-1}. The NMR spectra of D_2O saturated solution were recorded with a Bruker unit at room temperature. TMS was used as an internal reference.

To calculate optimized geometric structures, a few quantum mechanical *ab initio* methods were used: (i) Hartree–Fock (HF), (ii) the density functional theory (DFT) hybrid method B3PW91, which uses the Becke's three-parameter functional with non-local correlation provided by the Perdew-Wang 91 expression and (iii) the DFT hybrid method B3 LYP with non-local correlation provided by the Lee–Yang–Parr expression. The calculation was carried out with two functional bases: 6–311++G** (for atoms H–Kr) and LANL2DZ (for atoms H–Ba, La–Bi). All theoretical calculations were performed using the Gaussian 98W package of programs[21] running on a PC.

Experimental spectra were interpreted in terms of calculated data from DFT at the B3PW91/6–311++G** level. Theoretical wavenumbers were calculated according to the equation $\nu_{scaled} = 0.955\nu_{calculated} + 25.7$.[22] The chemical shifts were calculated using the GIAO (gauge including atomic orbitals) method at the B3PW91/6–311++G** level. Chemical shifts (δ_i) were calculated by subtracting the appropriate isotopic part of the shielding tensor (σ_i) from that of TMS (σ_{TMS}): $\delta_i = \sigma_{TMS} - \sigma_i$ (ppm). The isotropic shielding constants for TMS calculated using the same basis set at the B3PW91/6–311++G** level were equal to 31.8676 ppm for the ^1H nuclei and 187.2388 ppm for the ^{13}C nuclei.[21]

Additionally, the AIM theory of Bader[23] was used to localize bond critical points and to calculate their properties: electron densities at bond critical points ($\rho_{RCP}S$) and electron densities at ring critical points ($\rho_{RCP}S$). All AIM calculations[24,25] were performed using the AIM2000 program.[26]

The aromaticity indices (*HOMA*, *GEO*, *EN*, I_6) were calculated for optimal geometric structures of picolinates.[27–30]

The *HOMA* (harmonic oscillator model of aromaticity) index differs from all other geometry-based ones by assuming another reference bond length.[27–29] In this model, instead of the mean bond length, a concept of the optimal bond length is applied:

$$HOMA = 1 - \frac{\alpha}{n}\sum (R_{opt} - R_i)^2$$

where n is the number of bonds taken into account, α is an empirical constant chosen to give $HOMA = 0$ for the hypothetical Kekulé structure of benzene and $HOMA = 1$ for the system with all bonds equal to the optimal value R_{opt}, R_{opt} is a length of the CC bond for which the energy of the compression to the length of a double bond and expansion to the length of a single bond in 1,3-butadiene is minimal (the same procedure can be applied to bonds with heteroatoms) and R_i is an individual bond length. Within the confines of the HOMA model, it is possible to obtain two components which describe different contribution to a decrease in aromaticity, i.e. (a) due to bond elongation (the *EN* component) and (b) due to bond length alternation (the *GEO* component). Hence the final equation for *HOMA* is

$$\begin{aligned} HOMA &= 1 - \left[\alpha(R_{opt} - R_{av})^2 + \frac{\alpha}{n}\sum (R_{av} - R_i)^2\right] \\ &= 1 - EN - GEO \end{aligned}$$

where

$$GEO = \frac{\alpha}{n}\sum (R_{av} - R_i)^2$$

and

$$EN = \alpha\left(R_{opt} - R_{av}\right)^2$$

The value of the *HOMA* index is equal 1 for the entirely aromatic system, $HOMA = 0$ when the structure is non-aromatic and $HOMA < 0$ for an anti-aromatic ring.[27–29]

I_6, the Bird aromaticity index, is defined as

$$I_6 = 100[1 - (V/V_k)$$

where

$$V = (100/N_{av}) \cdot \left[\sum_{r=1}^{n} (N_r - N_{av})^2/n\right]^{\frac{1}{2}}$$

and

$$N = \frac{a}{R^2} - b$$

R is the observed bond length, N_r is the individual bond order, N_{av} is the mean bond order, n is the number of bonds and V_k, a and b are constants.[30] Bird's index can be used for hetero- and carbocyclic systems.

RESULTS AND DISCUSSION

Structure of picolinic acid and sodium picolinate

According to an x-ray diffraction study,[31] PA in a crystalline state takes the intermediate form between the neutral molecule and zwitterion. The molecules are linked by two symmetric minimum double hydrogen bonds, i.e. N—H—N and O—H—O, with a small potential barrier.[32]

The C═O bond length indicates that this bond does not possess a full double bond character, but the asymmetric stretching ν_{as}(C═O) band is observed in the IR spectrum of PA at 1720 cm^{-1}.

Theoretical calculations at the B3PW91/6–311++G** level performed for an isolated molecule of PA indicate that the most stable structure contains intramolecular hydrogen bonding between the hydrogen of the carboxylic group and the nitrogen atom in the ring [Fig. 1(c)]. According to these criteria, we can say that an H-bond exists if the electron density at the H···Y bond critical point is in the range 0.002–0.035 au. Based on Bader's AIM theory,[23] a critical point was found between the hydrogen atom of the carboxylic group and the nitrogen atom in the PA ring. The electron density was calculated as 0.031 au and confirms the presence of intramolecular hydrogen bonding between the atoms considered. The ring critical point value is 0.027 au (Fig. 2).

Bond lengths and angles in the compared structures of PA quantified theoretically (neutral molecules and zwitterion) and obtained experimentally from x-ray diffraction are given in Table 1. Geometric aromaticity indices, *HOMA*[27–29] and Bird's I_6,[30] were also calculated for both structures. As can be seen in Table 1, there is good compatibility between the experimental data and theoretically calculated bond lengths, angles and aromaticity indexes. Considerable differences occur only in the case of the *EN* aromatic index.

The most stable structure for sodium picolinate was found using the B3LYP/6–311++G** data basis set. The results of the calculations are given in Table 2 (intramolecular distances, aromaticity indices and angles) (Fig. 3).

FT-IR and Raman spectra

In Tables 3 and 4, the wavenumbers, intensities and assignments of the bands occurring in the vibrational spectra of the studied picolinates are given. The spectral assignment was based on literature data[2,32,33] and theoretical calculations.[21]

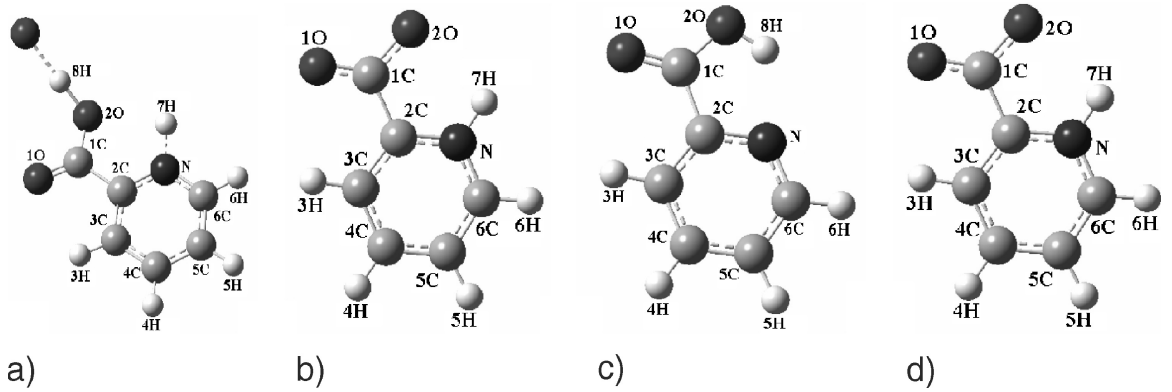

Figure 1. Crystallographic (a) and theoretically by calculated structures (b)–(d) for picolinic acid

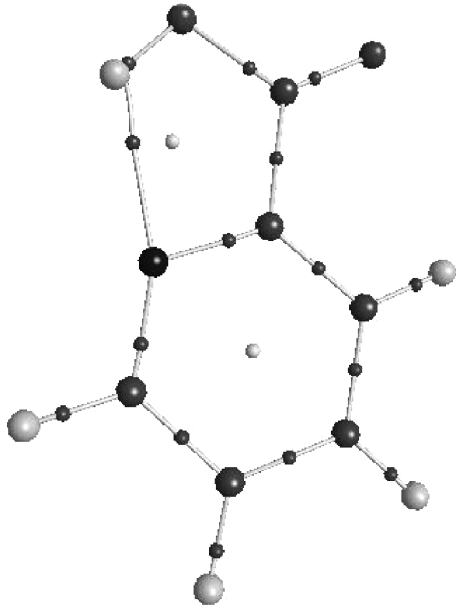

Figure 2. Location of bond critical points and ring critical points for the theoretical (most stable) structure of Picolinic acid

The bands in the spectra were divided into two groups: (i) those connected with carboxylic anion vibrations and (ii) those connected with aromatic ring vibrations.

In the first group, characteristic wide and intense bands responsible for the asymmetric [$\nu_{as}(COO^-)$: 1629–1610 cm^{-1} IR spectra, 1626–1617 cm^{-1} Raman spectra] and symmetric [$\nu_s(COO^-)$: 1397–1393 cm^{-1} IR spectra, 1410–1391 cm^{-1} Raman spectra] stretching of the carboxylic anion were observed.

The bands assigned to the symmetric in-plane deformation of the carboxylic anion (β_{sym}: 856–840 cm^{-1} Raman spectra, 849–840 cm^{-1} IR spectra) and asymmetric in-plane deformation of the carboxylic anion were present (β_{as}: 525–521 cm^{-1} Raman spectra, 548–516 cm^{-1} IR spectra). The bands connected with the aromatic ring vibration [ν(CC), ν(CH), β(CH), γ(CH) and γ(CC)] were observed in the whole spectral range (4000–400 cm^{-1}).

The influence of the metal on the vibrational structure of the carboxylic anion bands in the series Li → Na → K → Rb → Cs were small, but a characteristic

Table 1. Distances (Å), angles (°), dipole moments, energies and aromaticity indices for picolinic acid (experimental and theoretical, Fig. 1)

	Experimental[31]	Theoretical (B3PW91/6–311++G**)		
	Structure (a)[a]	Structure (b)	Structure (c)	Structure (d)
Distances (Å)[b]				
C1—C2	1.51	1.56	1.51	1.50
C2—C3	1.37	1.39	1.39	1.39
C3—C4	1.38	1.39	1.39	1.39
C4—C5	1.37	1.40	1.39	1.39
C5—C6	1.38	1.38	1.39	1.39
C6—N	1.34	1.40	1.33	1.33
N—C2	1.35	1.34	1.34	1.33
C1—O1	1.21	1.23	1.20	1.21
C1—O2	1.28	1.25	1.33	1.34
O2—8H	0.80	—	—	—
N—7H	0.91	1.06	0.99	0.97
Angles (°)[b]				
C2—C3—C4	119.9	118.5	117.9	118.2
N1—C2—C3	120.4	119.2	123.6	123.7
C4—C5—C6	118.7	119.0	118.8	118.5
O2—C1—O1	126.8	134.3	123.1	123.1
C2—N1—C6	120.0	124.4	118.6	117.4
C3—C4—C5	119.3	120.4	118.9	118.6
N1—C6—C5	121.8	118.6	122.6	123.5
Dipole moment (D)	—	10.7053	5.9430	2.4873
Energy (hartree)[c]	—	−436.7853	−436.8128	−436.8067
Geometric aromaticity indices[d]				
HOMA	0.948	0.991	0.997	0.996
GEO	0.004	0.008	0.001	0.003
EN	0.047	0.000	0.002	0.001
I_6	81.50	83.29	85.21	87.88

[a] The average estimated standard deviation of the carbon–carbon bond lengths is <0.005 Å.
[b] The atoms are numbered as in Fig. 1.
[c] 1 hartree = 2625.500 kJ mol^{-1}.
[d] *HOMA*, harmonic oscillator model of aromaticity (*HOMA* = 1 − *EN* − *GEO*); *GEO*, geometric contribution to the aromaticity; *EN*, energetic contribution to the aromaticity; I_6, Bird index, which describes the geometric contribution to the aromaticity.

Table 2. Distances (Å), angles (°), dipole moments, energies and geometric aromatic indices calculated for sodium picolinate using three theoretical methods

	HF/6–311++G**	B3PW91/6–311++G**	B3LYP/6–311++G**
Distance[a]			
C2—N7	1.32	1.33	1.34
N7—C6	1.32	1.33	1.33
C6—C5	1.39	1.39	1.39
C5—C4	1.38	1.39	1.39
C4—C3	1.38	1.39	1.39
C3—C2	1.39	1.40	1.40
C1—C2	1.52	1.52	1.52
C1—O8	1.25	1.27	1.27
C1—O9	1.23	1.26	1.26
O8—Na10	2.21	2.22	2.22
O9—Na10	2.20	2.21	2.21
Angle[a]			
C2—N7—C6	118.4	117.7	117.9
N7—C6—C5	123.5	123.8	123.7
C6—C5—C4	118.0	118.2	118.2
C5—C4—C3	118.7	118.6	118.6
C4—C3—C2	118.6	118.8	118.9
C3—C2—C1	119.2	119.1	119.2
N7—C2—C1	118.1	118.1	118.1
C2—C1—O8	116.8	116.6	116.7
C2—C1—O9	119.4	119.2	119.3
O8—C1—O9	123.8	124.2	124.0
O8—Na10—O9	60.4	60.5	60.7
Dipole moment (D)	5.6207	5.6997	5.5030
Energy (hartree)	−595.7500	−598.5201	−598.7443
Geometric aromaticity indices			
HOMA	0.979	0.992	0.987
GEO	0.007	0.003	0.003
EN	0.230	0.005	0.010
I_6	87.48	85.49	85.23

[a] The atoms are numbered as in Fig. 3.

and general tendency might be observed. The wavenumbers of the bands $\beta_s(COO^-)$ in the IR spectra and $\nu_{as}(COO^-)$ and $\nu_s(COO^-)$ in the Raman spectra show a general decreasing trend in the series $Li \rightarrow Na \rightarrow K \rightarrow Rb \rightarrow Cs$. The wavenumbers of the $\nu_{as}(COO^-)$ and $\beta_{as}(COO^-)$ bands in the IR spectra and $\beta_s(COO^-)$ in the Raman spectra show a general decreasing trend (except for the Rb complex). The wavenumbers of the $\nu_s(COO^-)$ band in the IR spectra do not show any tendency.

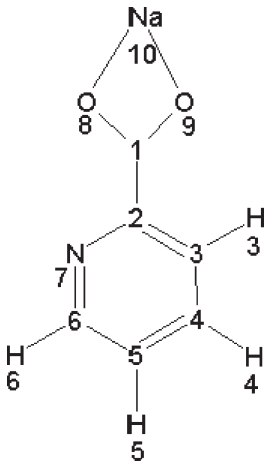

Figure 3. Atom assignments for sodium picolinate

The wavenumbers of the ν_s, ν_{as}, β_s and β_{as} bands were correlated with three parameters: electronegativity, ionic potential and the reverse atomic mass. The wavenumbers of these bands except ν_{as} correlate linearly with all factors tested at the statistically important level. For the symmetric stretching, the correlation coefficients are 0.83, 0.93 and 0.91 for electronegativity, ionic potential and reverse atomic mass, respectively. The correlation coefficients for the asymmetric stretching are small. The correlation coefficients for the symmetric in-plane deformation are 0.92, 0.98 and 0.96 for electronegativity, ionic potential and reverse atomic mass, respectively. Appropriate linear equations are $y = 76.9x + 778.5$, $y = 1924.7x + 828.3$ and $y = 114.2x + 839.9$ for electronegativity, ionic potential and reverse atomic mass, respectively. The correlation coefficients for the asymmetric in-plane deformation are 0.83, 0.94 and 0.95 for electronegativity, ionic potential and reverse atomic mass, respectively. Analysis of the correlation coefficients shows that none of metal parameters examined relates at the same high level to change in wavenumber of all

Table 3. Experimental (IR, Raman) and theoretical IR wavenumbers (B3PW91/6–311++G**) (cm^{-1}) for picolinic acid and lithium, sodium and potassium picolinates[a]

Picolinic acid				Lithium picolinate				Sodium picolinate				Potassium picolinate				Assignment and normal mode of the aromatic ring[33]	
Calculated[b] IR[c]		Exp. IR	Exp. Raman	Calculated IR[c]		Exp. IR	Exp. Raman	Calculated IR[c]		Exp. IR	Exp. Raman	Calculated IR[c]		Exp. IR	Exp. Raman		
Wavenumber	Intensity	Wavenumber	Wavenumber	Wavenumber	Intensity	Wavenumber	Wavenumber	Wavenumber	Intensity	Wavenumber	Wavenumber	Wavenumber	Intensity	Wavenumber	Wavenumber		
3102	1.94	3113m	3113w	3104	2.42	—	—	3103	2.89	—	—	3102	3.17	—	—	$\nu(CH)_{ar}$	20b
3089	6.44	—	3092w	3081	15.62	—	—	3079	19.60	—	—	3077	2.75	—	—	$\nu(CH)_{ar}$	
3072	5.92	—	3058vw	3067	9.12	3061w	3064w	3059	11.13	3062w	3063w	3056	12.3	3046m	3056w	$\nu(CH)_{ar}$	7b
—	—	—	—	—	—	1629s	—	—	—	1617vs	1626w	—	—	1611vs	1617vw	$\nu_{as}(COO^-)$	
1599	7.92	1595s	1596w	1591	23.52	1589s	1591w	1593	115.89	1586vs	1590m	1598	184.89	1585s	1586m	$\nu(CC)_{ar}$	8a
1582	13.29	1573m	1574w	1585	18.32	1567s	1567vw	1585	48.89	1566vs	1571w	1586	37.18	1565s	1566w	$\nu(CC)_{ar}$	8b
1461	17.23	1455s	1442vw	1465	24.36	1476w	1478vw	1459	3.06	—	1475w	1458	2.11	1467vw	1467w	$\nu(CC)_{ar}$	19a
1436	70.16	1439m	—	1419	22.29	1443m	1445w	1416	0.27	1439s	1440w	1415	0.62	1422m	1432w	$\nu(CC)_{ar}$	19b
—	—	—	—	—	—	1397vs	1410w	—	—	1394vs	1400w	—	—	1396vs	1398m	$\nu_s(COO^-)$	
1309	18.33	—	—	1292	11.8	1240w	—	1289	9.35	1235w	1239w	1288	8.87	1230w	1231w	ν(C-N)	
1282	5.14	1198s	1238vw	1279	10.22	1170w	1175vw	1277	11.57	1169w	1172w	1276	12.81	1167w	1168w	β(CH)	
1222	4.45	—	—	1162	6.38	1147w	1147vw	1159	7.65	1145w	1050m	1159	6.86	1143w	1142w	β(CH)	
1144	2.06	1086s	1087vw	1137	0.96	—	1090vw	1134	1.18	1089w	1090w	1133	1.08	1086w	1093w	β(CH)	18b
1090	3.32	1045s	1051w	1085	7.40	1044w	1047w	1082	6.75	1045w	1050m	1082	6.85	1045m	1046m	β(CH)	18a
—	—	—	—	—	—	849w	856w	—	—	844m	847m	—	—	841m	841m	$\beta_s(COO^-)$	
669	6.94	704s	694vw	720	6.94	702m	704vw	711	24.77	711m	703w	720	36.29	705s	699w	ϕ(CC)	6a
629	7.16	630m	631vw	628	42.07	631w	629vw	625	4.97	626w	628w	625	5.07	621w	621w	ϕ(CC)	6b
—	—	—	—	—	—	548w	—	—	—	—	527w	—	—	516vw	521w	$\beta_{as}(COO^-)$	

[a] ν, stretching; β, in-plane deformation; ϕ, out-of-plane deformation; v, very strong; s, strong; m, medium; sh, shoulder; w, weak.
[b] Fig. 1(c).
[c] $\nu_{scaled} = 0.955\ \nu_{calculated} + 25.7$.[22]

carboxylic anion vibrations. This means that the analysis of these data in such a way does not provide an answer as to which of the proposed metal parameters is most important in view of the influence of the metal on the vibrational structure of carboxylic anion. Principal component analysis was performed on wavenumbers of the four above mentioned bands (ν_s, ν_{as}, β_s and β_{as}).

The wavenumbers of the aromatic 19b bands in the Raman spectra (except for the caesium complex) show a decreasing tendency and wavenumbers of the other aromatic bands do not change systematically (scatter) along the metal series. The shift of the aromatic bands (regular and irregular) expresses the influence of the metal on the vibrational structure of the aromatic rings. The wavenumbers of the 19a, 19b, 9a, 8a and 8b bands were correlated with the same metal parameters as in case of wavenumbers of the bands related to carboxylic anion vibration. The correlation coefficients for the 18a and 18b bands are very small and statistically unimportant. The correlation coefficients for the 19a bands were 0.74, 0.67 and 0.59 for electronegativity, ionic potential and reverse atomic mass, respectively. For the 19b band the correlation coefficients were 0.86, 0.86 and 0.79 for electronegativity, ionic potential and reverse atomic mass, respectively.

The correlation coefficients for the 8b bands were 0.94, 0.97 and 0.91 for electronegativity, ionic potential and reverse atomic mass, respectively. For the 8a band the correlation coefficients were 0.80, 0.95 and 0.98 for electronegativity, ionic potential and reverse atomic mass, respectively. The correlation coefficients for the 9a bands were 0.90, 0.91 and 0.85 for electronegativity, ionic potential and reverse atomic mass, respectively. The wavenumbers of the ν(C–N), 6a and 6b bands do not correlate with any of the metal parameters studied.

The wavenumbers of some other bands reflecting vibration of the aromatic ring were analysed to estimate the influence of the coordinated metal on the uniform electronic charge distribution around the aromatic ring. However, the differences between correlation coefficients obtained for electronegativity, ionic potential and reverse atomic mass were too small to say which of the tested parameters is mostly responsible for the influence of the metal on the vibrational structure of the aromatic ring.

Principal component analysis

Principal component analysis (PCA) is a well-known statistical technique which produces linear combinations of the original data to reduce the number of input data. That is, PCA is a factor analysis technique that reduces the dimensions of a set of variables by reconstructing them into uncorrelated combinations (one can use PCA whenever uncorrelated linear combinations of variables are of use). The first principal component produced accounts for the largest amount of the input data variance. The second principal component accounts for the next largest amount of variance, and so on, until the total sample is combined into component groups. Each succes-

Table 4. Experimental IR and Raman wavenumbers (cm^{-1}) for rubidium and caesium picolinates

Rubidium picolinate		Caesium picolinate		Assignment and normal mode of the aromatic ring[33]
Raman	IR	Raman	IR	
3062w	3045m	3062w	3045w	$\nu(CH)_{ar}$ 7b
—	1610vs	—	1612vs	$\nu_{as}(COO^-)$
1587w	1585vs	1586w	1585s	$\nu(CC)_{ar}$ 8a
1562vw	1565vs	1567w	1565s	$\nu(CC)_{ar}$ 8b
1472vw	1466w	1471w	—	$\nu(CC)_{ar}$ 19a
1430vw	1422m	1434w	—	$\nu(CC)_{ar}$ 19b
1391w	1396vs	1391w	1393s	$\nu_s(COO^-)$
1235vw	1229w	—	1231w	ν(C–N)
1167w	1167vw	1166w	1166w	β(CH)
1136w	1149vw	1146w	1149w	β(CH)
1091vw	1086w	1089w	1086w	β(CH) 18b
1042vw	1044m	1049w	1045w	β(CH) 18a
842vw	840s	840w	840m	$\beta_s(COO^-)$
697vw	698s	699w	698m	ϕ(CC) 6a
623vw	621m	622w	621w	ϕ(CC) 6b
525vw	520vw	—	518vw	$\beta_{as}(COO^-)$

sive component explains progressively smaller portions of the variance in the total sample. All of the components are uncorrelated with each other, assuming that the obtained principal components represent variability of the input data which are small in number.

PCA was performed on the data obtained from the IR experiment. Wavenumbers of the 8a, 8b, 19a, 19b and 9a bands were analysed. The PCA procedure extracted two principal components. Together they account for 86.25% of the variability in the original data. The FPC (first principal component) accounts for 63.86% and the second for 22.39%. The principal components and their weights are given in Table 5. The components obtained, treated as characteristic for changes in electronic charge distribution along the series of analysed compounds, were correlated with different parameters: ionic potential, atomic mass, reverse atomic mass and electronegativity of the studied alkali metals. There is no correlation at a statistically important level between the second principal component and any of studied parameters. On the other hand, for FPC the correlation coefficients are 0.89, -0.60, 0.80 and 0.60 for ionic potential, atomic mass, reverse atomic mass and electronegativity, respectively. This observation confirms that ionic potential is the main parameter responsible for changes in electronic charge distribution in the aromatic ring.

A similar procedure was performed on wavenumbers of the carboxylic anion band, $\nu_{as}(COO^-)$, $\nu_s(COO^-)$, $\beta_s(COO^-)$ and $\beta_{as}(COO^-)$, to estimate changes in the electronic charge distribution in this part of molecule. The first and second principal components are given in the Table 6 together with appropriate weights. Again, correlations were established between the studied parameters and the obtained statistical data. Once again the highest correlation coefficients were obtained for ionic potential (0.99) and for reverse atomic mass (0.97). This means that ionic potential is the most important parameter of the metal influencing the electronic charge distribution in the molecule.

Theoretical IR spectra

Wavenumbers of IR vibrations for PA and for lithium, sodium and potassium picolinates were calculated. Wavenumbers of the chosen spectral bands are compared with those calculated theoretically at the B3PW91/6–311++G** level in Table 3. Wavenumbers obtained theoretically were scaled up according to the equation $\nu_{scaled} = 0.955\nu_{calculated} + 25.7$.[22] Comparison of the calculated band wavenumbers with those obtained experimentally gave satisfactory results.

Aromaticity indices of alkali metal picolinates

The structures of lithium, sodium, potassium, rubidium and caesium picolinates at the B3PW91/LANL2DZ level were calculated. Additionally, the structures of lithium, sodium and potassium picolinates at the B3PW91/6-311++G** level were calculated as well.[21] Based on the geometric data for the analysed compounds, geometric indices of aromaticity were calculated.[27–30] Comparison of the geometric index values for PA and its derivatives with alkali metals is shown in Table 7.

From the results obtained we conclude that heavier metals, such as rubidium and caesium, perturb the aromatic system of the acid to a greater extent than light metals, such as lithium and sodium. Perturbation increases generally in the series Li → Cs. With increasing atomic number of the coordinated metal, its energetic contribution to ring dearomatization increases (*EN*[27,28]), whereas the geometric contribution remains the same (*GEO*[27–29]). The *HOMA* and I_6 values show a tendency to increase. More precise calculations can be obtained using

Table 5. First and second principal components and their weights obtained for alkali metal picolinates using wavenumbers of the 8a, 8b, 19a, 19b and 9a bands

Compound	First principal component	Band	Weight	Second principal component	Band	Weight
Li picolinate	2.24	8a	0.52	−0.21	8a	−0.33
Na picolinate	1.52	8b	0.38	−0.28	8b	0.36
K picolinate	−1.64	19a	0.50	0.13	19a	−0.24
Rb picolinate	−1.57	19b	0.55	−1.28	19b	0.03
Cs picolinate	−0.55	9a	0.16	1.64	9a	0.84

the 6–311++G** function base,[21] but this base does not contain data for rubidium and caesium. To compare the whole set of investigated metal complexes, calculations with the less precise database LANL2DZ were performed; this database includes all H–Ba and La–Bi atoms. The aromaticity of the analysed compounds remains similar, but one can observe a distinct decreasing trend in the order Li → Cs for geometric indices, which was also confirmed by the spectroscopic results presented in this paper.

NMR spectra

The theoretical and experimental NMR data for picolinates are given in Tables 8 (^{1}H NMR) and 9 (^{13}C NMR).

The NMR assignment was based on literature data.[34,35] The chemical shifts of protons (^{1}H NMR) and carbons (^{13}C NMR) in the series of studied alkaline metals express the influence of different metals on the electronic charge around those atoms.

^{1}H NMR spectra

When we replaced a hydrogen atom with metal we observed a decrease in chemical shifts compared with the ligand. This is evidence for an increase in the electron density around protons (screen effect). The protons' chemical shifts show a general decreasing tendency in the series of Li → Na → K → Rb. Caesium has higher values of chemical shifts than rubidium (Table 8). The aromaticity shows a general decreasing tendency in the series of HPic → Li → Na → K → Rb (increasing destabilization of the aromatic system). Values of the proton 3, 4 and 5 signals show a general decreasing tendency in the series Li → Na → K → Rb (Table 8). Values of the proton 6 signals change irregularly. The greatest differences in the chemical shifts of the investigated complexes compared with the ligand can be observed for proton 6.

The smallest differences in chemical shifts for all protons compared with the ligand were observed for lithium picolinate; higher values were observed for the other picolinates.

^{1}H chemical shifts were calculated using the GIAO method at the B3PW91/6–311++G** level for optimized structures of Li, Na, and K picolinates and PA. Theoretical values of the chemical shifts of the analysed nuclei were deducted from the difference in the shield tensor trace of TMS and the examined compound.[22] The theoretical values of the chemical shifts obtained were compared with the experimental values versus TMS (Table 8). Good correspondence was found for the calculated and experimentally obtained chemical shifts of protons 6 and 4 (Fig. 2). In case of the chemical shifts of protons 3 and 5 (Fig. 2), no satisfactory correlation between the experimental and theoretical results was found. Experimental chemical shift values of protons 5 were found to be much higher than the theoretical values for the respective complexes. The greatest difference between the experimental and theoretical shift values for protons 3 was found for the potassium complex (1.51 ppm). In the case of protons 3, higher values of the calculated than the experimental chemical shifts were found. For the chemical shifts of protons 4 and 6 no differences greater than 0.5 ppm were found between the

Table 6. First and second principal components and their weights obtained for alkali metal picolinates using wavenumbers of the $\nu_{as}(COO^-)$, $\nu_s(COO^-)$, $\beta_s(COO^-)$ and $\beta_{as}(COO^-)$

Compound	First principal component	Band	Weight component	Second principal	Band	Weight
Li picolinate	2.55	$\nu_{as}(COO^-)$;	0.38	−0.56	$\nu_{as}(COO^-)$;	0.68
Na picolinate	0.58	$\nu_s(COO^-)$;	0.32	1.56	$\nu_s(COO^-)$;	−0.73
K picolinate	−0.83	$\beta_s(COO^-)$	0.62	−0.77	$\beta_s(COO^-)$	0.02
Rb picolinate	−0.95	$\beta_{as}(COO^-)$	0.61	−1.03	$\beta_{as}(COO^-)$	−0.05
Cs picolinate	−1.35			0.80		

Table 7. Aromaticity indices for alkali metal picolinates

	EN		*GEO*		*HOMA*		I_6 (Bird)	
B3PW91	LANL2DZ	6–311++G**	LANL2DZ	6–311++G**	LANL2DZ	6–311++G**	LANL2DZ	6–311++G**
Picolinic acid[a]	0.098	0.002	0.003	0.001	0.889	0.997	83.80	85.21
Lithium picolinate	0.114	0.004	0.002	0.003	0.882	0.993	83.98	85.59
Sodium picolinate	0.119	0.004	0.002	0.004	0.879	0.992	83.94	85.57
Potassium picolinate	0.118	0.004	0.003	0.003	0.879	0.993	83.81	85.37
Rubidium picolinate[b]	0.119	—	0.003	—	0.878	—	83.93	—
Caesium picolinate[b]	0.125	—	0.003	—	0.872	—	83.91	—

[a] Fig. 1(c).
[b] Basis 6–311++G** not obtained for rubidium and caesium atoms.

Table 8. Theoretical (B3PW91/6–311++G**) and experimental ^{1}H chemical shifts (δ, ppm) for lithium, sodium, potassium, rubidium and caesium picolinates and picolinic acid

	Picolinic acid				Picolinate[a]									
	Structure (a)	Structure (b)	Structure (c)	Structure (d)	Lithium		Sodium		Potassium		Rubidium		Caesium	
Proton	Exp.	Theor.			Exp.	Theor.	Exp.	Theor.	Exp.	Theor.	Exp.	Theor.	Exp.	Theor.
3	7.62	8.69	8.53	8.65	7.42	8.74	7.33	8.72	7.22	8.73	7.19	—	7.24	—
4	7.96	8.35	8.06	7.92	7.89	7.83	7.77	7.75	7.67	7.72	7.64	—	7.68	—
5	8.05	7.57	7.61	7.55	8.00	7.38	8.00	7.29	7.8	7.23	7.76	—	7.82	—
6	8.70	8.05	8.70	9.01	8.47	9.05	8.50	8.99	8.44	8.91	8.42	—	8.46	—

[a] The atoms are numbered as in Fig. 3.

Table 9. Theoretical (B3PW91/6–311++G**) and experimental ^{13}C chemical shifts (δ) for lithium, sodium, potassium, rubidium and caesium picolinate and picolinic acid

	Picolinic acid				Picolinate[a]									
	Structure (a)	Structure (b)	Structure (c)	Structure (d)	Lithium		Sodium		Potassium		Rubidium		Caesium	
Carbon	Exp.		Theor.		Exp.	Theor.	Exp.	Theor.	Exp.	Theor.	Exp.	Theor.	Exp.	Theor.
1	166.25	156.24	166.45	171.25	167.61	187.24	167.65	181.15	—	179.89	168.18	—	168.46	—
2	149.46	158.73	153.24	153.25	156.06	158.98	157.71	161.05	—	161.49	159.17	—	158.82	—
3	137.59	130.53	128.81	131.84	137.48	131.39	136.29	131.30	—	130.25	135.56	—	135.69	—
4	124.74	150.15	143.18	140.85	123.42	140.30	123.35	139.70	—	138.98	122.72	—	122.92	—
5	127.15	128.07	131.60	131.32	124.62	129.56	123.44	128.51	—	127.51	123.12	—	123.26	—
6	148.41	137.19	152.77	155.27	147.63	155.87	148.17	155.35	—	154.38	147.85	—	147.87	—

[a]The atoms are numbered as in Fig. 3.

experimental and theoretical values for the investigated complexes.

^{13}C NMR spectra

The investigated complexes contain the carboxylic anion. The presence of an oxygen atom in this group causes an increase in the chemical shift of the carbon atom band. This is evidence for a decrease in the electron density around this atom. Analysis of the chemical shift values of the metal complexes compared with the ligand shows an increasing tendency for the C-1 and C-2 carbon atoms (Fig. 2); for other signals it shows a decreasing tendency (Table 9). The electron densities around the C-1 atom are lower than for other carbon atoms, which is why we see the largest chemical shift values for this atom. The changes in the chemical shift values for the carbons of picolinates are not regular. The chemical shift values for C-1 and C-2 show an increasing tendency in the series Li < Na < Rb < Cs (Table 9). The signal values for C-3, C-4 and C-5 show a decreasing tendency (except for the caesium complex).

^{13}C chemical shifts were calculated using the GIAO method at the B3PW91/6–311++G** level for optimized structures of Li, Na, and K picolinates and PA. Theoretical values of the chemical shifts of the analysed nuclei were deducted from the difference in the shield tensor trace of TMS and the examined compound.[22] The theoretical values of the chemical shifts obtained were compared with the experimental values versus TMS.

Good correspondence was found for the calculated and experimentally obtained chemical shifts of carbon atoms C-2, C-3, C-5 and C-6 (Fig. 2). In the case of C-1 and C-4, considerable differences between the calculated and experimentally obtained chemical shift values were observed.

CONCLUSIONS

The type of carboxylic anion structure and character of the metal–ligand bond influence the structure and electron charge distribution in the aromatic ring.

The investigation on the structure of alkali metal picolinates proved that Rb and Cs cations perturb the electron charge distribution in PA to a greater extent than the light metals Na and K.

Calculated aromaticity indices (*HOMA*, I_6) confirm that heavy metals perturb the electronic charge distribution more than light metals. Although the differences in aromaticity indices are small, the general trend Li < Na < K < Rb < Cs is noticeable.

The changes in aromaticity (uniform electronic charge distribution) were confirmed by ^{1}H and ^{13}C NMR data.

Analysis of the correlation between the wavenumber of one chosen band in the IR spectrum and analysed metal parameters (ionic potential, electronegativity,

mass) did not give any unambiguous answer as to which parameter determines the perturbation of the electronic charge distribution. The answer to this question was not obtained until we applied PCA. The PCA results imply that the ionic potential of the metal is the parameter that influences' the electronic charge distribution to the greatest-extent.

There is an intramolecular bond between the nitrogen atom and hydrogen atom of the carboxylic group in the most stable structure of PA. This conclusion is based on data from the Bader theory (AIM).

Acknowledgements

This work was supported financially in part by the Polish State Committee for Scientific Research (Grant No. 6 PO6T 08521) and the Bialystok Technical University (theme No. W/II/31/03 and I/IIŚ/24/04). The authors are grateful to Professor Nina Sadlej-Sosnowska and Dr Ewa Regulska for helpful discussions.

REFERENCES

1. Koczon P, Piekut J, Borawska M, Lewandowski W. *J. Mol. Struct.* 2003; **651–653**: 651–656.
2. Koczon P, Dobrowolski JCz, Lewandowski W, Mazurek AP. *J. Mol. Struct.* 2003; **655**: 89–95.
3. Koczon P, Hrynaszkiewicz T, Swislocka R, Samsonowicz M, Lewandowski W. *Vib. Spectrosc*. 2003; **33**: 215–222.
4. Lewandowski W, Baranska H. *Vib. Spectrosc*. 1991; **2**: 211–220.
5. Lewandowski W, Fuks L, Kalinowska M, Koczon P. *Spectrochim. Acta A* 2003; **59**: 3411–3420.
6. Koczon P, Lewandowski W, MoScibroda P, Priebe W, Wieckowska E. *Can. J. Appl. Spectrosc*. 1996; **41**: 144–149.
7. Bajdor K, Koczon P, Wieckowska E, Lewandowski W. *J. Inf. Quantum Chem*. 1997; **62**: 385–392.
8. Lewandowski W. *J. Inorg. Chem.* 1992; **8**: 303–310.
9. Lewandowski W, Baranska H, MoScibroda P. *J. Raman Spectrosc*. 1993; **24**: 819–824.
10. Lewandowski W. *J. Mol. Struct*. 1983; **101**: 93–103.
11. Liang Y, Noda LK, Sala O. *J. Mol. Struct*. 2000; **554**: 271–277.
12. Stearns DM, Armstrong WH. *Inorg. Chem*. 1992; **31**: 5178–5184.
13. Song R, Kim KM, Sohn YS. *Inorg. Chim. Acta* 1999; **292**: 238–243.
14. Chakov NE, Collins RA, Vincent JB. *Polyhedron* 1999; **18**: 2891–2897.
15. Ding H, Olson LK, Caruso JA. *Spectrochim. Acta, Part B* 1996; **51**: 1801–1812.
16. Hepburn DD, Burney JM, Woski SA, Vincent JB. *Polyhedron* 2003; **2**: 455–463.
17. Stearns DM, Silveira SM, Wolf KK, Luke AM. *Mutat. Res*. 2002; **513**: 135–142.
18. Morris GS, Guindry KA, Hegsted M, Hasten DL. *Nutr. Res*. 1995; **15**: 1045–1052.
19. Liang Y, Noda LK, Sala O. *J. Mol. Struct*. 2000; **554**: 271–277.
20. Dazzi C, Candiano G, Massazza S, Ponzetto A, Varesio L. *J. Chromatogr. B* 2000; **75**: 61–68.
21. Frisch MJ, Trucks GW, Schlegel HB, Scuseria GE, Robb MA, Cheeseman JR, Zakrzewski VG, Montgomery JA, Stratmann RE, Burant JC, Dapprich S, Millam JM, Daniels AD, Kudin KN, Strain MC, Farkas O, Tomasi J, Barone V, Cossi M, Cammi R, Mennucci B, Pomelli C, Adamo C, Clifford S, Ochterski J, Petersson GA, Ayala PY, Cui Q, Morokuma K, Malick DK, Rabuck AD, Raghavachari K, Foresman JB, Cioslowski J, Ortiz JV, Baboul AG, Stefanov BB, Liu G, Liashenko A, Piskorz P, Komaromi I, Gomperts R, Martin RL, Fox DJ, Keith T, Al-Laham MA, Peng CY, Nanayakkara A, Gonzales C, Challacombe M, Gill PMW, Johnson B, Chen W, Wong MW, Andres JL, Head-Gordon M, Replogle ES, Pople JA. *Gaussian 98, Revision A.7*. Gaussian: Pittsburgh, PA, 1998.
22. Rode JE, Dobrowolski JCz, Jamróz M, Borowiak MA. *Vib. Spectrosc*. 2001; **250**: 133–149.
23. Bader RFW. *Atoms in Molecules: A Quantum Theory*. Oxford University Press: New York, 1990.
24. Biegler-König FW, Bader RFW, Tang YH. *J. Comput. Chem*. 1982; **3**: 317–328.
25. Bader RFW, Tang YH, Tal Y, Biegler-König FW. *J. Am. Chem. Soc.* 1984; **104**: 946–952.
26. Biegler-König F. *AIM2000*. University of Applied Sciences: Bielefeld.
27. Krygowski TM, Cyranski MK. *Chem. Rev.* 2001; **101**: 1385–1419.
28. Krygowski TM. *J. Chem. Inf. Comput. Sci*. 1993; **33**: 70–78.
29. Krygowski TM, Cyranski MK. *Tetrahedron* 1996; **52**: 10255–10264.
30. Bird CW. *Tetrahedron* 1985; **41**: 1409–1418.
31. Hamazaki H, Hosomi H, Takeda S, Kataoka H, Ohba S. *Acta Crystallogr., Sect. C* 1998; **54**: IUC9800049.
32. Park SM, Kim K, Kim MS. *J. Mol. Struct*. 1995; **344**: 195–203.
33. Versanyi G. *Assignments for Vibrational Spectra of 700 Benzene Derivatives*. Akadémiai Kiadó: Budapest, 1973.
34. Broadburst CL, Schmidt WF, Reeves JB, Polansky MM, Gautschi K, Anderson RA. *J. Inorg. Biochem*. 1997; **66**: 119–130.
35. Kingry KF, Royer AC, Vincent JB. *J. Inorg. Biochem*. 1998; **72**: 79–88.